Scripta Materialia 139 (2017) 104–107

Contents lists available at ScienceDirect

Scripta Materialia

journal homepage: www.elsevier.com/locate/scriptamat

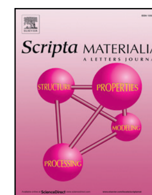

Regular article

PdGe contact fabrication on Se-doped Ge

M. Descoins [a], J. Perrin Toinin [a], S. Zhiou [a], K. Hoummada [a], M. Bertoglio [a], R. Ma [b], L. Chow [b], D. Narducci [c], A. Portavoce [a,*]

[a] IM2NP, CNRS/Aix-Marseille University, Faculté des Sciences de Saint-Jérôme case 142, 13397 Marseille, France
[b] Department of Physics, University of Central Florida, Orlando, Florida 32816, USA
[c] Department of Materials Science, University of Milano-Bicocca, via R. Cozzi 55, 20125, Milano, Italy

A R T I C L E I N F O

Article history:
Received 22 December 2016
Received in revised form 12 June 2017
Accepted 15 June 2017
Available online xxxx

Keywords:
Germanium
Palladium
Selenium
Contact
Reaction

A B S T R A C T

PdGe contact fabrication on Se-doped Ge(001) is investigated. PdGe thin film resistivity is two times lower if the PdGe layer is grown by Pd reactive diffusion on Se-doped Ge, compared to PdGe layer grown in the same condition on Se-free Ge. The phase sequence and the phase growth kinetics during Pd reactive diffusion with Ge are not modified by the presence of Se atoms. However, the PdGe film texture is different with Se, and Se segregates at the PdGe/Ge interface. These results suggest that Se atoms may be used to produce efficient contacts on *n*-type Ge.

© 2017 Acta Materialia Inc. Published by Elsevier Ltd. All rights reserved.

Si-based complementary metal oxide semiconductor (CMOS) technology development allowed continuous microelectronic device size reduction, combined with the continuous improvement of microelectronic device efficiency (speed, power consumption…). CMOS technology allows highly integrated, high-performance, and high-reliability microelectronic chips to be produced at relatively low-cost and high yield. To carry out this constant improvement, materials used to build and to connect transistors were changed or modified several times over the years from technology node to technology node. For example, Co was changed to Ni for silicide ohmic contacts [1–3], SiO_2 was changed to HfO_2 for gate dielectric [4–5], and Cu replaced Al for metallic interconnections [6–8]. Si was kept as the base semiconductor so far, but with the size limits insuring transistor standard operations soon being reached, different semiconductors other than Si should be used in future transistors in order to support device improvements [9–10]. Among them, Ge appears as a plausible choice, since Ge has faster charge carrier mobilities and is fully compatible with CMOS technology [11–16]. Ge was first introduced in the CMOS technology for heterojunction bipolar transistor fabrication, for low power high-frequency radio-frequency applications [17–19]. Today, complementary transistor technology uses *n*-type transistors with a Si channel stressed by SiGe source and drain, and *p*-type transistors with a SiGe channel [20–25]. In addition, Ge-based devices such as photodetectors are now integrated in Si photonics integrated circuits [26]. However, Ge-based CMOS technology suffers two major limitations: i) low *n*-type doping levels [27], and ii) the difficulty to produce ohmic contacts on *n*-type Ge [28–33]. PdGe is expected to be one of the best materials for ohmic contact fabrication on Ge due to its low resistivity and reduced Ge consumption [34]. Reactive diffusion of a thin Pd film on intrinsic Ge has been already studied aiming to design a self-aligned germanide process similar to the Salicide process used in Si CMOS technology [34–41]. Pd_2Ge was shown to grow first, and to be followed by the growth of PdGe. PdGe experiences an agglomeration process at relatively low temperature [39]. In the present work, the formation of a PdGe contact on *n*-type Se-doped Ge was investigated comparing with a PdGe film formed in the same condition on the same Ge substrate not doped with Se.

Ga-doped Ge(001) substrates exhibiting a resistivity between 0.059 and 0.088 Ω cm were implanted with a dose of 3.6×10^{15} Se at cm^{-2} with an energy of 130 keV, and annealed under vacuum (4×10^{-5} Torr) in a commercial rapid thermal annealing (RTA) setup at 700 °C for 30 min in order to activate Se atoms. Secondary ion mass spectrometry (SIMS) was used to determine the Se distribution in the sample using a CAMECA IMS 3F setup with a 3 keV O_2^+ ion beam, and Hall Effect electrical measurements were performed to measure the concentration of free carriers in the sample after activation. Then, a 20-nm thick polycrystalline Pd film was deposited at room temperature (RT) on the sample surface using a commercial magnetron sputtering system with a base pressure of 10^{-8} Torr. Pd was sputtered from a 99.99% pure Pd target using a 99.9999% pure Ar gas flow in the DC mode. Then, the sample was loaded in an X-ray diffraction (XRD) setup and was in situ annealed under vacuum (10^{-6} Torr) following a heating ramp consisted of 5 °C per minute steps separated by 5 min-

* Corresponding author.
E-mail address: alain.portavoce@im2np.fr (A. Portavoce).

http://dx.doi.org/10.1016/j.scriptamat.2017.06.029
1359-6462/© 2017 Acta Materialia Inc. Published by Elsevier Ltd. All rights reserved.

long XRD measurements at constant temperature (T), corresponding to an average ramp of ~1.7 °C min^{-1}. The XRD measurements were performed between RT and 400 °C in the Bragg-Brentano geometry, using a Cu K_α source ($\lambda_{K\alpha} = 0.154$ nm). XRD pole figures were also acquired at RT with steps of 2° after the in situ measurements using a focalized Cu K_α source. The atomic distribution in the sample was analyzed by atom probe tomography (APT) after annealing using a CAMECA LEAP 3000X-HR system. APT measurements were performed in the laser mode at $T = 20$ K with a laser energy of 0.15 nJ, a laser pulse frequency of 100 kHz, and an evaporation rate of 0.2%. The PdGe film resistivity was measured using the four probe technique and compared to the resistivity of a PdGe film grown in the same condition on the same Ge substrate but not doped with Se. The PdGe resistivity (ρ) was averaged over 15 measurements performed on different locations on the same film.

Fig. 1 presents the Se SIMS profiles measured in the Ge(001) substrate after Se implantation (open triangles) and after the activation annealing performed at 700 °C for 30 min (open squares). The Se distribution corresponds to a Gaussian distribution after implantation, with a maximum concentration of ~5×10^{20} at cm^{-3} located at ~60 nm below the sample surface. Se atoms diffused during activation annealing, decreasing this maximum to ~1×10^{20} at cm^{-3}. The average doping level measured in this sample by the Hall effect technique was found to be ~3.3×10^{19} electrons cm^{-3}, which corresponds to a Ge resistivity of ~7.7×10^2 μΩ cm [42]. One note that Se atoms being considered as double donors [43], the electron concentration is expected to correspond to an average Se concentration of only ~1.65×10^{19} at cm^{-3} that is close to our APT detection limit [44–46]. Se concentrations higher than this limit correspond to inactive Se atoms, probably incorporated in Se-Ge clusters. Fig. 2a displays the evolution of the diffractogram measured in situ versus T during the ramp annealing of the [20-nm thick Pd/Se-doped Ge(001)] sample. As expected [37–38, 40], the phase formation sequence is sequential with the formation of only two phases: first Pd_2Ge and second PdGe. A single diffraction peak is detected after Pd deposition at the diffraction angle 2θ ~ 40°, corresponding to the Pd(111) atomic planes. The diffraction intensity of this peak decreases during annealing until total extinction, while the intensity of the Pd_2Ge(111) and Pd_2Ge(002) peaks (2θ ~ 37.5° and 53.7°, respectively) increases simultaneously from zero up to a maximum, resulting from the Pd layer consumption during the Pd_2Ge layer growth. Similarly, the consumption of the Pd_2Ge layer during the growth of PdGe leads to the decrease of Pd_2Ge(111) and Pd_2Ge(002) peak intensities, with the concomitant intensity increase of five new peaks corresponding to PdGe (2θ ~ 29.3°, 33.2°, 41.7°, 43°, and 52.5°, consistent with PdGe (101), (111), (211), (121), and (002) planes, respectively). A single PdGe layer is in contact with the Ge substrate at the end of the experiment. The observed diffraction peaks of all the phases are similar to those observed during the reaction of a Pd film on a Se-free

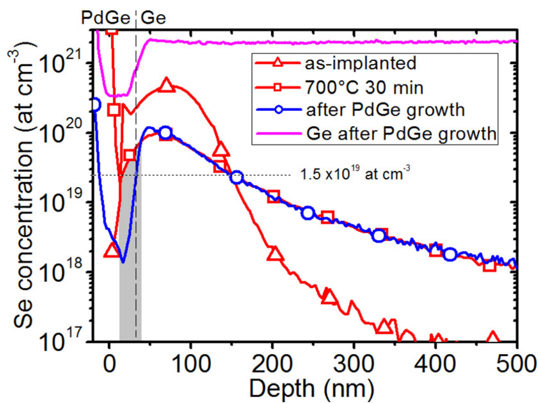

Fig. 1. Se SIMS profiles measured in the Se-implanted Ge(001) substrate before (open triangles) and after (open squares) activation annealing, as well as in the PdGe/Se-doped Ge sample after an annealing ramp of ~1.7 °C min^{-1} up to 400 °C (open circles).

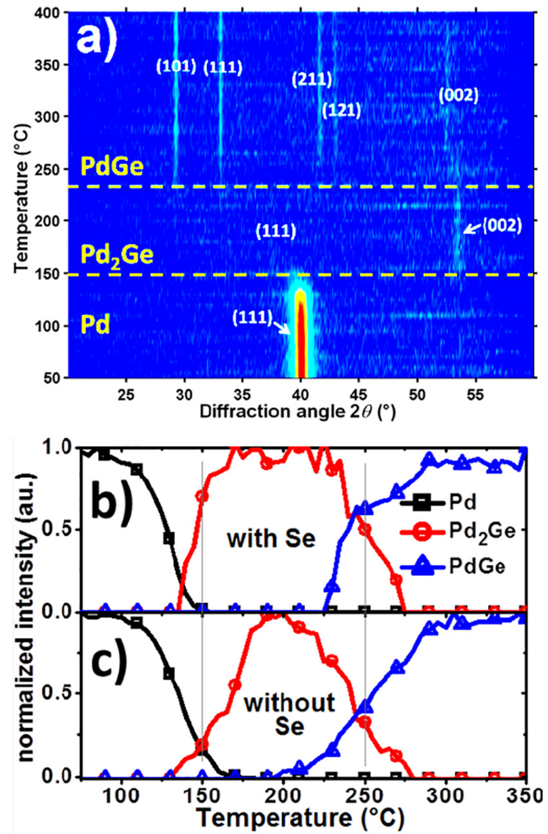

Fig. 2. a) In situ XRD measurements performed on the Se-doped sample; b) and c) integrated and normalized Pd(111), Pd_2Ge(002) and PdGe(101) diffraction peaks recorded during in situ XRD annealing of a Pd layer deposited either on a Se-doped Ge substrate (b) or on a Se-free Ge substrate (c).

Ge(001) substrate [41]. Fig. 2b and c present the variation versus T of integrated and normalized diffraction peaks corresponding to the most intense peak of each phase present in the phase sequence with and without Se: the Pd(111), Pd_2Ge(002), and the PdGe(101) peaks. Based on the Pd(111) peak decrease, Pd_2Ge growth is observed to start at T ~ 115 °C with Se, which is similar to the case of Pd reaction on the Se-free Ge substrate [40]. PdGe growth starts at T ~ 225 °C, which is close to what is observed with the Se-free Ge substrate [40]. Fig. 3a presents XRD measurements performed at RT after annealing, on the PdGe layer grown on the Se-doped substrate (open squares), as well as on a PdGe layer grown in the same conditions on a Se-free substrate (open circles). The main diffraction peaks are the same for the two samples. The most intense diffraction peaks correspond to the PdGe (101) and (111) planes. These planes do not exhibit the highest XRD structure factor (41% and 48.5%, respectively). Consequently, these diffractograms do not correspond to an entirely random texture. The texture of the PdGe layers was investigated using XRD pole figure measurements performed for the PdGe (211), (121), and (101) planes. Fig. 3b and c present the (121) pole figures obtained on the samples with and without Se, respectively. A random-like signal is detected in the two cases (background intensity in Fig. 3b and c). However, the measurements show that the strongest diffraction intensity results from the axiotaxial texture PdGe(121)//Ge(220) in the Se-free sample, while it corresponds to the epitaxial texture PdGe(001)//Ge(001) in the sample with Se. These two types of texture were already reported between PdGe and Ge [47]. Consequently, Se doping does not modify the phase sequence and the phase growth kinetics during Pd reaction with the Ge substrate, but promotes an epitaxial texture instead of an axiotaxial texture. The resistivity measurements performed on the PdGe films grown either on the Se-doped Ge substrate or the Se-free Ge substrate show significant differences. The resistivity of the PdGe film grown on the Se-

Download English Version:

https://daneshyari.com/en/article/5443434

Download Persian Version:

https://daneshyari.com/article/5443434

Daneshyari.com